CHAPTER 4

TD-DFT Study of Absorption and Emission Spectra of 2-(2′-Aminophenyl)benzothiazole Derivatives in Water

4.1 Introduction

Intracellular sulfur-containing molecules are involved in many crucial processes in animals and humans. Known biomolecules of the type include glutathione (GSH), cysteine (Cys) and homocysteine (Hcy) [71, 114]. Beside these traditional organic examples recent studies also found that the toxic hydrogen sulfide (H_2S) can be produced under cellular regulation and function as a signaling gasotransmitter next to nitric oxide (NO) and carbonmonoxide (CO) [72]. In mammals, H_2S is so far found to be released from lungs, livers, kidneys, pancreases, hearts and brains via the breakdown of Cys and Hcy [73, 74, 76, 77, 153]. Imbalance of H_2S quantity in cells could lead to serious physiological malfunctions such as Alzheimer's disease, impaired cognitive ability, gastric mucosal, injury and hypertension [78, 114]. Therefore, the development of H_2S monitoring methods is considered highly important in tackling with these illnesses.

Fluorescent dyeing provides an efficient approach for the H_2S detection. In recent years, several probing strategies for intracellular H_2S have been explored, for instance, copper sulfide precipitation, necleophilic substitutions by H_2S, oxidation of selenoxides and reductions of nitro ($-NO_2$) and azido ($-N_3$) compounds. The last tactic has been actively studied because the azido group can react promptly with H_2S and turn into amino ($-NH_2$) group, while remaining inert against other GSH and other thiols. When attached to a fluorophore the azido group normally turns off the fluorescence due to its ability to quench the excited state of the adjacent fluorophore. Upon the reduction into an amine, the fluorophore suppression terminates and a glow can be observed [71, 79, 114]. So far, several azido fluorogenic probes have been reported, mainly based on

ลิขสิทธิ์มหาวิทยาลัยเชียงใหม่
Copyright© by Chiang Mai University
All rights reserved

well-known fluorophores such as coumarins [11, 12], anthracenes [154], naphthalimide [81], luminol [80] or borondipyrromethene (BODIPY) [13, 155]. However, not every azido dye works well with probing in vivo for a number of challenges. Besides the high sensitivity and fluorescent intensity, the probes are required to have low levels of self absorption caused by the overlapping of their own absorption and emission bands. Another main challenge is that the probes must emit lights in long wavelengths, preferably in the reddish or near-infrared side of the spectrum as the interference by normal pigments in tissues is low in this region [114].

Compounds in phenylbenzathiazole family have been extensively studied as fluorophores, especially ones with intramolecular hydrogen bonds which conserve the planarity of the conjugated system. 2-(2´-hydroxyphenyl)benzathiazole (HBT) is probably one of the most widely studied due to its ability to undergo the excited-state intramolecular proton transfer (ESIPT), which promotes large Stokes' shift and thus favours the use as analytical fluorophore [128, 156, 157]. Photophysics studies on their heteroatom-substituted siblings, namely benzoxazole and benzimidazole, have also been carried out due to their simplicity in syntheses and modifications [60, 132, 158]. The amino derivative of HBT called 2-(2´-aminophenyl)benzathiazole (APBT) has also been studied for decades and shown potential in applications as molecular probes. The earliest works coming from Dogra's group also suggest occurrence of ESIPT in APBT but only in aprotic solvents [159, 160]. Such behavior suggests no proton transfer in APBT in cellular environment. Combination of phenylbenzathiazole derivatives with azido-amino conversion strategy in molecular probing has just emerged recently. In 2014, Jiang et al. proposed an azido dye which releases HBT upon the reduction by H_2S. This resulted in the detection limit of 2.4 micromolar when applied to detect H_2S in HeLa cells [161]. And around the same time, Zhang and Guo reported 2-(2′-azidophenyl)benzathiazole (AzPBT) as a very efficient probe. When reacted with H_2S and turned into its amino product, APBT, it expresses a 1150-fold fluorescence at the wavelength of 450 nm with high quantum yield. The detection limit was found to be as low as 0.78 nanomolar when used to detect H_2S in B16 cells [86].

Theoretical calculations of excited state properties of molecules are crucial tools in obtaining better understanding and guiding designs of dyes and pigments. It has been

ลิขสิทธิ์มหาวิทยาลัยเชียงใหม่
Copyright© by Chiang Mai University
All rights reserved

accepted in general that density functional theory (DFT) [95, 98, 162] and time-dependent density functional theory (TD-DFT) [163] are capable of providing good estimates of spectroscopic properties, including fluorescence spectra, of several families of organic dyes [164-168]. Computational studies of APBT emerged shortly after the discovery of its applications as a molecular probe. In 2015, the tuning of the spectrum of APBT by addition of substituents has been attempted. It was learnt from the time-resolved experiments in adjunct with quantum mechanical calculations that the presence of strong electron withdrawing tosyl group on the amino nitrogen can promote ESIPT which causes desirable Stokes' shift [169]. The latest update from the same group went further and revealed the fate of keto product of ESIPT which has multiple possibilities including keto emission and intersystem crossing [170].

In this work, we applied TD-DFT with hybrid functionals in investigating the effects of carbon-attached substituents on the absorption and emission spectra of APBT derivatives. The results of this study are expected to lead to a general guideline in modifying APBT and similar molecules towards more efficient fluorescent probes for H_2S in physiological environment (i.e. in water). The substituents studied in this work include only two different groups: cyano (−CN) group, representing electronwithdrawing groups (EWG), and dimethylamino ($-NMe_2$) group, representing electron-donating groups (EDG). However, the combination of these two groups at different three positions on the APBT core results in a series of different compounds that features different direction of push-pull architecture.

4.2 Computational Details

Ground-state optimizations of APBT and APBT04 structures were performed using density functional theory (DFT) methods with four different hybrid exchange functionals, namely B3LYP [95-97], PBE0 [99], M06 and M06-2X [100]. All calculations were run with 6-311+G(d,p) basis set. Dielectric constants of water (for APBT) and dichloromethane (for APBT04) were taken into account by using SCRF method through the nonequilibrium polarizable continuum model calculations (CPCM) framework to confirm the consistency with available data [86, 169]. The global minimum of all ground-state geometries was confirmed by the absence of imaginary frequencies.

ลิขสิทธิ์มหาวิทยาลัยเชียงใหม่
Copyright© by Chiang Mai University
All rights reserved

Vertical excitation energies of APBT in water and APBT04 in dichloromethane were then computed for 4 electronic states using TD-DFT methods and translated to absorption spectra. Next, the optimization of the first excited states of the two compounds with varied exchange-correlation functionals were carried out to obtain the starting point for the emissive transition. Then, again, vertical emission energies were predicted by TDDFT. The outcome absorption and emission spectra were then compared to the experimental results reported by Zhang et al. [86] for APBT in water and Tseng et al. [169] for APBT04 in dichloromethane. The contribution of molecular orbitals in the electronic transition were also calculated using the GaussSum3.0 program [43]. The exchange-correlation functional that gave the best fitted spectra to the experiments would then be chosen to calculate the spectra of the test molecules listed in Figure 4.1.

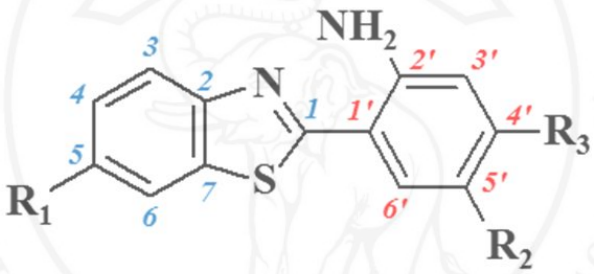

Code	Substituted position			Code	Substituted position		
	R_1	R_2	R_3		R_1	R_2	R_3
APBT	H	H	H	**APBT10**	H	NMe_2	H
APBT01	CN	H	H	**APBT11**	H	NMe_2	CN
APBT02	CN	H	NMe_2	**APBT12**	CN	CN	H
APBT03	CN	H	CN	**APBT13**	CN	CN	NMe_2
APBT04	H	CN	H	**APBT14**	CN	CN	CN
APBT05	H	CN	NMe_2	**APBT15**	CN	NMe_2	CN
APBT06	H	CN	CN	**APBT16**	NMe_2	CN	NMe_2
APBT07	NMe_2	H	H	**APBT17**	NMe_2	CN	CN
APBT08	NMe_2	H	NMe_2	**APBT18**	NMe_2	NMe_2	CN
APBT09	NMe_2	H	CN				

Figure 4.1 Molecular structures of 2-(2'-Aminophenyl)benzothiazoles (APBT) and its derivatives. R_1, R_2 and R_3 indicate the substitution positions used in this work.

From the calculated spectra, molecules with large Stokes' shifts and small overlaps of spectra would then be further studied for the chances of ESIPT from the amino proton towards the acceptor nitrogen on the thiazole ring. Ground- and excited-

ลิขสิทธิ์มหาวิทยาลัยเชียงใหม่
Copyright© by Chiang Mai University
All rights reserved

state potential energy curves (PECs) of the proton along the transfer path were constructed from the energy minimization with constrained distance between the donor nitrogen and proton. The constrained N–H distance was then varied (scanned) to obtain the minimal energy along the transfer path and the energy barrier of the proton transfer in both ground and excited states. These calculations were carried out in Gaussian 09 program [149].

4.3 Results and Discussion

4.3.1 Exchange-Correlation Functional Selection

The experimental and calculated maximum absorption (λ_{max}) wavelengths of APBT in water and APBT04 in dichloromethane with varied exchange-correlation functionals were listed in Table 4.1. Since two absorption maxima can be observed for both APBT derivatives, they were separately denoted as λ_1 and λ_2. The computed λ_1 and λ_2 from B3LYP functional appeared to be the most fitted to the selected experimental data in comparison to others, with only less than 10 nm deviations in wavelengths. Other hybrid functionals (M06, M06-2X and PBE0) tend to greatly overestimate excitation energies and thus give significantly shorter wavelengths in absorption spectra by at least 15 nm. This outcome supported the use of B3LYP functional for the spectra calculations of the other designed APBT derivatives.

Table 4.1 Available experimental absorption wavelengths compared to theoretical simulations for APBT and APBT04 in solution phase using different density functional theory (DFT) methods with hybrid exchange functional at 6-311+ G(d,p) basis set**.**

Method	APBT in H_2O (nm)		APBT04 in CH_2Cl_2 (nm)	
	λ_1	λ_2	λ_1	λ_2
TD-B3LYP	370	289	363	276
TD-M06	358	284	357	273
TD-M06-2X	326	255	330	253
TD-PBE0	357	279	268	254
Experiment	375 [86]	≃290 [86]	363 [169]	-

ลิขสิทธิ์มหาวิทยาลัยเชียงใหม่
Copyright© by Chiang Mai University
All rights reserved

4.3.2 Ground and Excited States of APBT and its Derivatives

Key geometric parameters of the optimised structures of studied APBT derivatives in ground and the first excited states are reported in Table 4.2. In general, the key bond lengths (C_1–C_1', C_2' –N and N–H bonds) are conserved in all molecules in their ground states. However, when excited, the C_1–C_1' and C_2' –N bonds slightly shrank by 0.01–0.04 Å. Such shrinkage matched the idea of classical resonance in the conjugated double bonds. Meanwhile, the N–H bond slightly lengthened in favour of proton donating by about 0.01 Å. The $NC_1C_1'C_2'$ dihedral angles remained low under 10 degrees in all studied compounds in both ground and excited states. This suggested that the benzothiazole and phenyl rings still remain co-planar, and that the conjugation systems of APBT derivatives are still intact in upon their first excitations.

Table 4.2 The selected bond lengths (Å) and dihedral angles (degree) for ground and excited state optimised structures calculated by B3LYP/6-311+ G(d,p) level of theory.

Code	Ground state (S_0)				Excited state (S_1)			
	C_1–$C_{1'}$	$C_{2'}$–N	N–H	$NC_1C_{1'}C_{2'}$	C_1–$C_{1'}$	$C_{2'}$–N	N–H	$NC_1C_{1'}C_{2'}$
APBT	1.45	1.36	1.01	1.74	1.43	1.34	1.02	0.00
APBT01	1.45	1.36	1.01	1.10	1.44	1.34	1.02	0.03
APBT02	1.45	1.36	1.01	1.22	1.44	1.35	1.02	0.00
APBT03	1.45	1.35	1.01	0.00	1.43	1.33	1.02	0.00
APBT04	1.46	1.35	1.01	0.01	1.42	1.33	1.02	0.00
APBT05	1.45	1.35	1.01	0.79	1.42	1.34	1.02	0.08
APBT06	1.46	1.35	1.01	0.01	1.42	1.34	1.02	0.00
APBT07	1.46	1.37	1.01	3.03	1.42	1.36	1.02	1.63
APBT08	1.45	1.37	1.01	1.95	1.43	1.35	1.02	5.99
APBT09	1.45	1.36	1.01	1.99	1.42	1.36	1.02	0.89
APBT10	1.45	1.37	1.01	3.99	1.44	1.35	1.02	4.04
APBT11	1.46	1.37	1.01	7.14	1.43	1.34	1.02	1.82
APBT12	1.46	1.35	1.01	0.00	1.43	1.33	1.02	0.00

ลิขสิทธิ์มหาวิทยาลัยเชียงใหม่
Copyright© by Chiang Mai University
All rights reserved

Table 4.2 (Continued)

Code	Ground state (S_0)				Excited state (S_1)			
	$C_1–C_{1'}$	$C_{2'}–N$	N–H	$NC_1C_{1'}C_{2'}$	$C_1–C_{1'}$	$C_{2'}–N$	N–H	$NC_1C_{1'}C_{2'}$
APBT13	1.46	1.35	1.01	1.03	1.43	1.34	1.02	0.61
APBT14	1.46	1.35	1.01	0.00	1.42	1.34	1.02	0.00
APBT15	1.45	1.36	1.01	1.95	1.43	1.34	1.02	1.42
APBT16	1.45	1.35	1.01	1.18	1.42	1.35	1.02	0.96
APBT17	1.46	1.35	1.01	0.00	1.42	1.35	1.02	0.00
APBT18	1.46	1.36	1.01	0.46	1.42	1.35	1.02	2.22

4.3.3 Absorption and Energy Band Gap of APBT Derivatives

The calculated absorption spectra of APBT derivatives at the TD-B3LYP/6-311+G(d,p) level are listed along with the calculated most probable transitions in Table 4.3. In terms of the probability in transition, the table shows that the dominant transition in every APBT derivative is the excitation from the highest occupied molecular orbitals (HOMOs) to the lowest unoccupied molecular orbitals (LUMOs), which represents the origin of the wavelength λ_1. The energy levels of HOMO and LUMO of each compound were visualise in Figure 4.2 and will be discussed simultaneously with Table 4.3.

The λ_1 wavelengths of most APBT derivatives are higher than 370 nm indicating the red shift in absorption when compared with APBT core. The only two exceptions are the APBT04 and APBT05 which have cyano groups (−CN) attached to the R_2 position while the R_1 position remained unsubstituted. Such patterns of the substitutions were predicted to give small blue shifts instead (having λ_1 at 363 and 364 nm respectively). The red shifts resulted from substituent effects are extraordinarily strong in compounds that possess But least one of these common features: 1) the attachment of -CN group at the R_3 position, and/or 2) dimethylamino ($-NMe_2$) group at the R_2 position. All the molecules that meets one of the two requirements were found to express absorption wavelengths longer than 450 nm with APBT6 being the only outlier (λ_1 = 388 nm). These findings can lead to a generalised idea for experimentalists that

ลิขสิทธิ์มหาวิทยาลัยเชียงใหม่
Copyright© by Chiang Mai University
All rights reserved

electron withdrawing groups (EWG) are desired at R_3 position, and that electron donating groups (EDG) are desired at R_2 position in order to synthesise APBT-derived dyes that absorb light at longer wavelengths which, in turn, fluoresce at longer wavelengths.

The absorption energy gaps visualised in Fig. 4.2 can also give useful information for synthetic strategy. It was observed that $–NMe_2$ group at R_1 position does not favour the red shift for APBT deducing from the unusual elevation of HOMO in APBT7, APBT8 and APBT16. However, this does not apply to APBT9, APBT17 and APBT18 as they are influenced by – CN group at R_3 position.

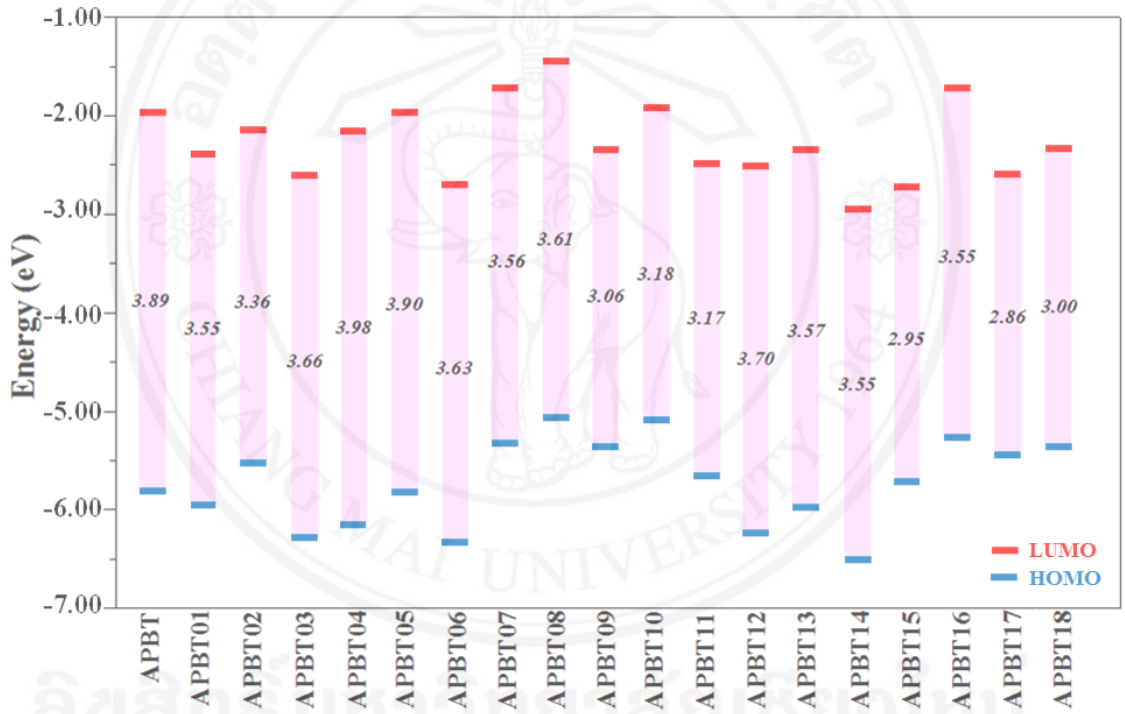

Figure 4.2 Calculated HOMOLUMO energy level diagram of APBT and its derivatives obtained from B3LYP/6-311+G(d,p) level.

ลิขสิทธิ์มหาวิทยาลัยเชียงใหม่
Copyright© by Chiang Mai University
All rights reserved

Table 4.3 Absorption wavelengths (nm), excitation energy (eV), oscillator strength (f) and major contributions (%) of APBT derivatives in water. The calculations were performed using B3LYP/6-311+ G(d,p) level**.**

Code	λ_1				λ_2			
	nm	**eV**	***f***	**MOs (%)**	**nm**	**eV**	***f***	**MOs (%)**
APBT01	403	3.07	0.424	H→L (99%)	314	3.94	0.329	H-1→L (83%)
APBT02	412	3.00	1.042	H→L (97%)	285	4.35	0.243	H-2→L (67%)
APBT03	459	2.70	0.366	H→L (99%)	331	3.74	0.512	H-1→L (88%)
APBT04	363	3.41	0.426	H→L (97%)	276	4.49	0.396	H→L+1 (67%)
APBT05	364	3.40	0.730	H→L (93%)	266	4.66	0.416	H→L+2 (48%)
APBT06	388	3.19	0.453	H→L (96%)	291	4.25	0.552	H→L+1 (72%)
APBT07	393	3.15	0.767	H→L (98%)	251	4.93	0.147	H-3→L (49%)
APBT08	387	3.20	1.170	H→L (98%)	283	4.38	0.107	H→L+3 (79%)
APBT09	452	2.74	0.780	H→L (99%)	280	4.42	0.155	H→L+2 (73%)
APBT10	458	2.70	0.189	H→L (99%)	311	3.98	0.444	H-1→L (85%)
APBT11	464	2.71	0.202	H→L (98%)	342	3.62	0.426	H-1→L (91%)
APBT12	389	3.18	0.469	H→L (98%)	265	4.67	0.313	H→L+3 (79%)
APBT13	395	3.13	0.887	H→L (95%)	274	4.52	0.401	H→L+3 (35%)
APBT14	401	3.09	0.501	H→L (97%)	295	4.20	0.496	H→L+1 (78%)
APBT15	500	2.47	0.226	H→L (99%)	351	3.53	0.486	H-1→L (87%)
APBT16	396	3.13	0.973	H→L (98%)	269	4.60	0.316	H→L+4 (41%)
APBT17	483	2.56	0.654	H→L (100%)	289	4.29	0.200	H→L+3 (47%)
APBT18	468	2.64	0.641	H→L (94%)	268	4.62	0.214	H-4→L (47%)

To further investigate the nature of the charge distribution and charge transfer in the excited state, the frontier molecular orbitals (the HOMOs and LUMOs) of APBT derivatives are depicted in Fig. 4.3. The electron densities in the HOMOs and LUMOs of the studies APBT derivatives suggested the π- to-π* character mixed with partial n-

ลิขสิทธิ์มหาวิทยาลัยเชียงใหม่
Copyright© by Chiang Mai University
All rights reserved

to-π* character. Intramolecular charge transfer (ICT) can also be noticed in some molecules, namely APBT03, APBT10, APBT11, APBT15 and APBT18. The existence of EDG (−NMe2) on the R_2 position is the common feature in these compounds. These could be the result of the strong electron-donating nature of the $–NMe_2$ functional group. The $–NMe_2$ at the R_1 position also contributed to the ICT characters in APBTs, but with relatively smaller extent, as seen in the molecular orbital plots of APBT07-09 and APBT16-18.

4.3.4 Emission Spectra and Stokes' Shift

In this section, we investigate the influence of substituent on absorption and emission spectra of APBT derivatives considering various substitution position. Table 4.4 listed the emission spectral data of APBT derivatives in water along with the major transitions of the emission. It was revealed that the dominant transition in the fluorescence of APBT derivatives are the transition from LUMOs to HOMOs of their ground states, with the only exception for APBT08 which has dominant transition from LUMO to HOMO-1 instead.

ลิขสิทธิ์มหาวิทยาลัยเชียงใหม่
Copyright© by Chiang Mai University
All rights reserved

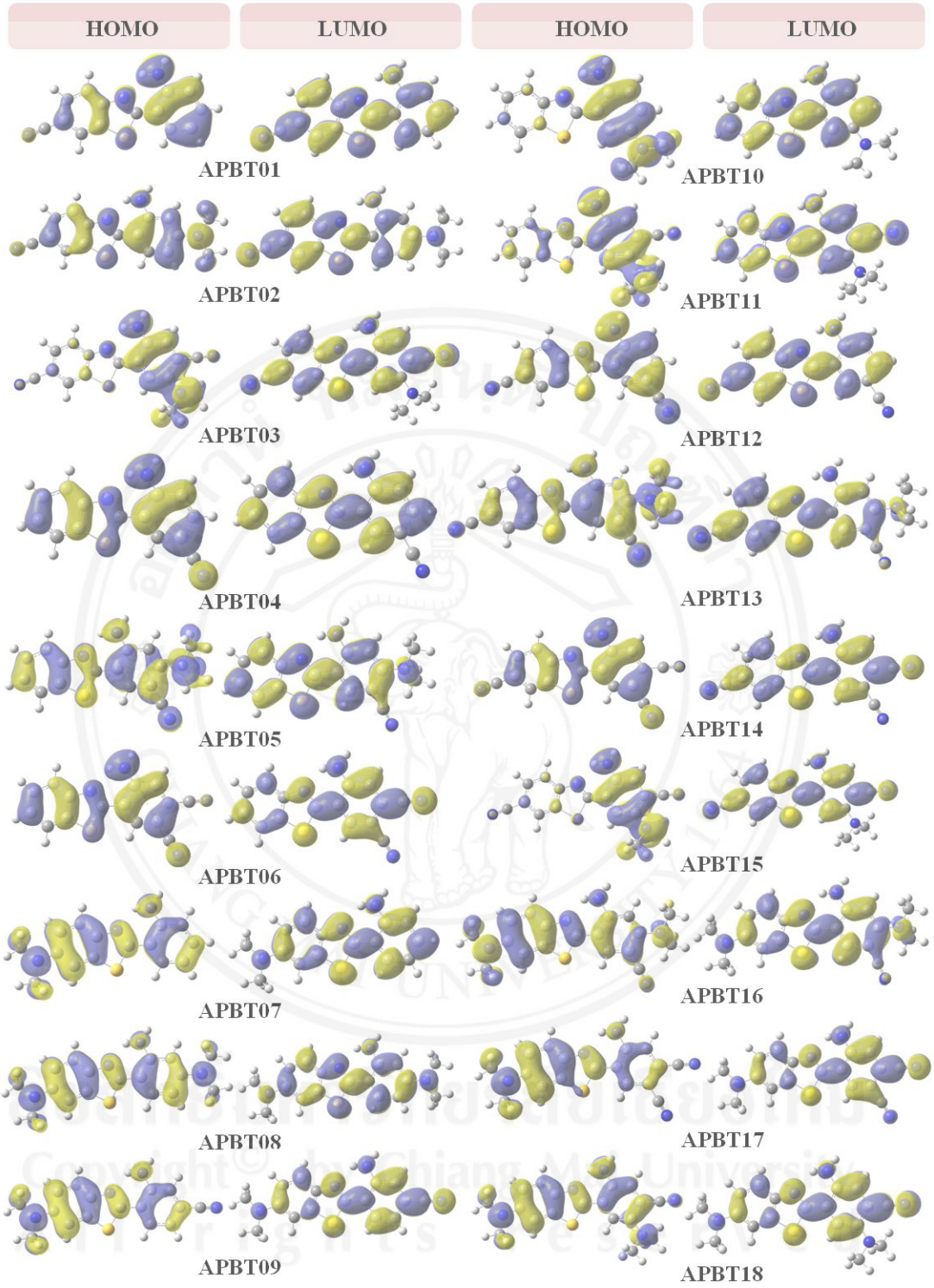

Figure 4.3 Frontier HOMO and LUMO molecular orbitals of APBT and its derivatives obtained from B3LYP/6-311+G(d,p) level**.**

Table 4.4 Emission wavelengths (nm), excitation energy (eV), oscillator strength (*f*) and major contributions (%) of APBT and its derivatives in water. The calculations were performed using B3LYP/ 6-311+G(d,p) level**.**

Code	λ_1				λ_2			
	nm	**eV**	***f***	**MOs (%)**	**nm**	**eV**	***f***	**MOs (%)**
APBT01	464	2.67	0.622	H→L (99%)	338	3.66	0.711	H-1→L (97%)
APBT02	435	2.85	1.074	H→L (97%)	289	4.29	0.242	H-2→L (44%)
APBT03	453	2.73	0.862	H→L (99%)	337	3.67	0.465	H-1→L (93%)
APBT04	424	2.92	0.750	H→L (99%)	294	4.21	0.491	H→L+1 (89%)
APBT05	429	2.89	1.199	H→L (98%)	327	3.79	0.241	H→L+1 (89%)
APBT06	462	2.68	0.808	H→L (98%)	314	3.94	0.652	H→L+1 (86%)
APBT07	451	2.74	0.865	H→L (99%)	325	3.81	0.046	H→L+1 (74%)
APBT08	466	2.66	0.439	H-1→L (71%)	344	3.60	0.625	H→L+1 (85%)
APBT09	546	2.27	1.185	H→L (99%)	395	3.13	0.077	H-1→L (97%)
APBT10	581	2.13	0.292	H→L (100%)	340	3.64	0.736	H-1→L (94%)
APBT11	631	1.96	0.260	H→L (100%)	375	3.03	0.834	H-1→L (96%)
APBT12	445	2.78	0.768	H→L (99%)	333	3.72	0.552	H-1→L (95%)
APBT13	451	2.79	1.382	H→L (97%)	321	3.86	0.222	H→L+1 (87%)
APBT14	469	2.64	0.864	H→L (99%)	315	3.93	0.570	H→L+1 (92%)
APBT15	699	1.77	0.268	H→L (100%)	379	3.27	1.000	H-1→L (97%)
APBT16	457	2.71	1.057	H→L (99%)	344	3.60	0.068	H-1→L (78%)
APBT17	502	2.46	0.621	H→L (99%)	303	4.09	0.190	H→L+3 (57%)
APBT18	607	2.04	0.483	H→L (99%)	475	2.61	0.711	H-1→L (98%)

In Figure 4.4, the simulated absorption (blue dashed line) and emission (continuous red line) spectra of APBT and its derivatives are shown. Discussing in combination with Table 4, it can be seen that the emission spectra of APBT11, APBT15 and APBT18 are the three compounds with strong fluorescence toward the reddish end

ลิขสิทธิ์มหาวิทยาลัยเชียงใหม่
Copyright© by Chiang Mai University
All rights reserved

of the visible light spectrum. All of their maximum emission wavelength (λ1) exceed 600 nm. The furthest red shift was observed in the calculated emission spectrum of APBT15 which gave λ1 as long as 699 nm. Regarding the emission wavelengths, the common features found in these APBT derivatives are 1) a strong EWG (CN) at R_3 position, combined with 2) a strong EDG (NMe_2) at R_2 position. Apart from the desirable emission wavelengths, these three molecules also gave large Stokes' shift with minimal overlap between the absorption and emission spectra, and in turn gave very small self-absorption when applied as fluorescent probes.

Another pattern of substitutions that exhibit interesting fluorescent spectra was the ones with –CN group at R_3 position and –NMe_2 group at R_1 position, namely APBT09 and APBT17, which gave the maximum fluorescence at 546 and 502 nm respectively. This pattern of substitutions can be inspected as a push-pull pattern where electrons pushed and pulled from the R_1 side to the R_3 side. However, APBT17 would not be appropriate to be used as a fluorescent probe due to its large overlap between the absorption and emission spectra.

APBT10 which has only –NMe_2 group at the R_2 position also gave a large Stokes' shift and has a maximum fluorescence close to the red region (λ_1 = 631 nm). This compound could as well serve as a good fluorescent probe.

ลิขสิทธิ์มหาวิทยาลัยเชียงใหม่
Copyright© by Chiang Mai University
All rights reserved

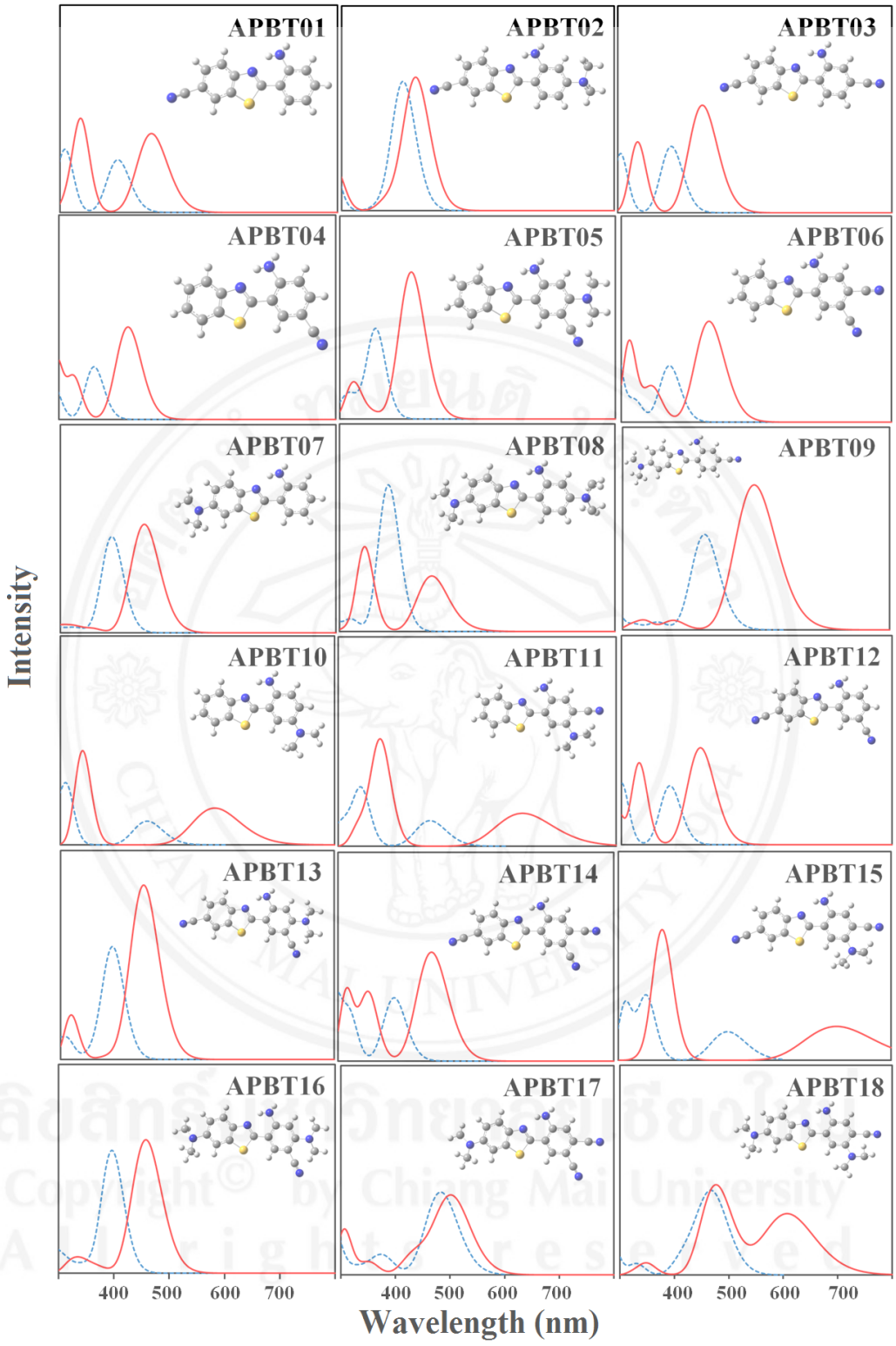

Figure 4.4 Simulated absorption (blue dashed line) and emission (red solid line) spectra of APBT and its derivatives by TD-B3LYP/ 6-311+G(d,p) in water.

ลิขสิทธิ์มหาวิทยาลัยเชียงใหม่
Copyright© by Chiang Mai University
All rights reserved

4.3.5 Potential Energy Curves of Proton Transfer

It must be noted that all of the previous discussions are based on the assumption that the ESIPT does not occur. In other words, the absorptions and emissions occur while the APBT derivatives remain in their enamine (E) form, and none of their imine (I) tautomeric counterparts are involved. In this section, the energy barriers (and thus the possibility) of the tautomerization from E form to I form in selected APBT derivatives (APBT, APBT04, APBT10, APBT11, APBT15 and APBT18) were estimated and discussed. The discussed compounds in this section were selected due to their outstanding fluorescent spectra in the earlier section.

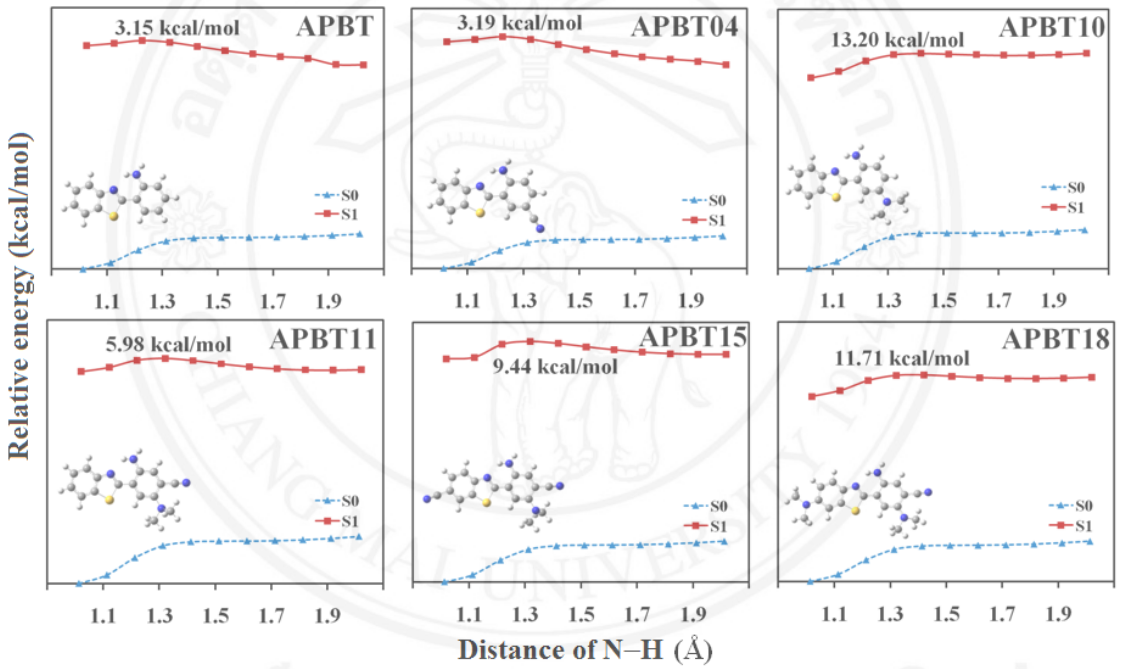

Figure 4.5 Potential energy curves of ground and excited states for selected derivatives with N–H bond length. The insert shows the corresponding optimized geometries

The ground and excited state structures of selected APBT derivatives were optimised in their corresponding electronic states with constrained N–H distance. The set of optimised energies at varied N–H distance were then used to construct a potential energy curve along the proton transfer path for each compound. This information was presented in Figure 4.5 to provide relative probability for the ESIPT process. From the figure, the energy of the ground state increases along with the lengthening of the N–H

ลิขสิทธิ์มหาวิทยาลัยเชียงใหม่
Copyright© by Chiang Mai University
All rights reserved

bond from the initial length without any local maxima. This suggested that the proton transfer from amino nitrogen to benzothiazolic nitrogen is rare or impossible for APBT derivatives in ground states. On the other hand, the excited state potential energy curves exhibit a barrier of 3.15, 3.19, 13.20, 5.98, 9.44 and 11.71 kcal/mol for APBT, APBT04, APBT10, APBT11, APBT15 and APBT18, respectively. Among these compounds, APBT and APBT04 had already been studied by experiments. In the 2014 work by Tseng et al., the ESIPT process is absence in APBTand very slow in APBT04. [37] From this information, we can make a deduction from the far higher energy barriers of the proton transfer that ESIPT process in APBT10, APBT11, APBT15 and APBT18 are unlikely, and probably impossible. Therefore, the emission spectra from these compounds are prone to exhibit single emission peaks from their E tautomers.

4.4 Chapter Summary

The effect of electron donating and withdrawing group are substituted on absorption and emission spectra of APBT derivatives was systematically investigated by TD-DFT/TDB3LYP/6-311+G(d,p) level. The calculated absorption wavelength of APBT derivatives from TD-B3LYP are in agreement with the experimental data. The result of the study revealed that these patterns of substitutions are likely to give fluorescent APBT-derived dyes with large Stokes' shifts:

1) A strong EDG at R_2 position and a strong EWG at R_3 position.
2) A push-pull architecture consisting of a strong EWG at R_1 position and a strong EDG at R_3 position.
3) Solely a strong EDG at R_2 position.

According to the results of the study, the derivative APBT11, APBT15 and APBT18 were proposed as potential candidates for the fluorescent probes for hydrogen sulfide in water or in cells. These three compounds were predicted to give fluorescence wavelengths at over 600 nm (orange to infrared region) solely from their enamine tautomer as deduced from the estimated energy barrier of the tautomerization. These rough generalised ideas, along with in depth understanding of the fluorescent of APBT, comprise a useful guideline toward the design of other fluorescent probes for this application.

ลิขสิทธิ์มหาวิทยาลัยเชียงใหม่
Copyright© by Chiang Mai University
All rights reserved